Abdominal Radiology (2019) 44:2147–2155
https://doi.org/10.1007/s00261-019-01963-y

HEPATOBILIARY

Liver metastases of neuroendocrine tumors: is it possible to diagnose different histologic subtypes depending on multiphasic CT features?

Basak Gulpinar[1] · Elif Peker[1] · Melahat Kul[1] · Atilla Halil Elhan[2] · Nuray Haliloglu[1]

Published online: 12 March 2019

Abstract

Purpose To assess and compare the multiphasic computed tomography (CT) features of neuroendocrine tumor (NET) liver metastases and to investigate the possibility to predict the histologic subtype of the primary tumor.

Materials and methods Between January 2013 and December 2017 patients with biopsy proven NET with at least one liver metastasis who underwent multiphasic CT were enrolled in this study. All cases were acquired using a standardized multiphasic liver CT protocol, arterial, portal, and hepatic venous phases were obtained. Images were retrospectively analyzed in consensus by two abdominal radiologists blinded to clinical data and histologic subtype. The size, number, and location of lesions were noted. Enhancement patterns of each lesion on arterial, portal, and hepatic venous phases were assessed. For quantitative analysis, CT attenuation of tumors, liver parenchyma, and aorta were measured using a circular region of interest (ROI) on arterial, portal, and hepatic venous phases for reflecting the blood supply of the tumor. Tumor-to-aorta and tumor-to-liver ratio were calculated in all three phases. Differences between subtypes of NET liver metastases were studied using ROC analysis of clustered data.

Results A total of 255 neuroendocrine tumor liver metastases divided into 101 (39.6%) pancreatic, 60 (23.5%) gastroenteric and 94 (36.8%) lung NET liver metastases were analyzed. Contrast enhancement of lesions was homogeneous in 78% of patients ($n=199$), which was significantly more frequent in patients with pancreatic group than in those with gastroenteric origin ($n=90$, 89.1% vs. $n=28$, 46.7%; $p<0.001$). Gastroenteric NET metastases frequently showed heterogeneous enhancement, which was significantly higher than in the other two groups (50% vs. 3% and 2%). With respect to the location of the primary tumor, the difference in enhancement patterns of the liver lesions was statistically significant ($p<0.001$). Pancreatic NET metastases were mostly hyperdense on arterial images and isodense on portal and hepatic venous phase images (79.2%, $n=80$). Gastroenteric NET metastases were mostly hyperdense on arterial phase images and hypodense on portal and hepatic venous phase images ($n=28$, 46.7%). The most frequent pattern for lung NET metastases was hypoattenuation on all three phase images ($n=44$, 46.8%). ROC analysis of clustered data revealed statistically significant differences between pancreatic NET liver metastases, gastroenteric NET liver metastases, and lung NET liver metastases in terms of tumor-to-aorta (T–A) ratio and tumor-to-liver (T–L) ratio ($p<0.001$).

Conclusion We observed statistically significant differences in multiphasic CT features (enhancement pattern, T–A ratio, and T–L ratio) between histologic subtypes of NET liver metastases. As the difference in histological subtypes of NET liver metastases results in a different prognosis and different management strategy, these CT features might help to identify the primary tumor when it is not known to ensure accurate tumor staging and to provide optimal treatment.

Keywords Neuroendocrine tumor · Liver · Metastases · Multiphasic CT · Enhancement pattern · Quantitative analysis

Introduction

Neuroendocrine tumors (NET) are epithelial neoplasms with predominant neuroendocrine differentiation arising from enterochromaffin cells. Variable clinical course and biological behavior can be seen in patients with NETs. Most NETs have endocrine function; they secrete

✉ Basak Gulpinar
basak.gulpinar@yahoo.com

[1] Department of Radiology, Ankara University School of Medicine, 06100 Ankara, Turkey

[2] Department of Biostatistics, Ankara University School of Medicine, 06100 Ankara, Turkey

neuroamines and peptides that can cause specific clinical syndromes; however, many are clinically silent until presentation with mass effects [1]. Primary tumors can arise in various organs; however, the gastrointestinal tract, pancreas, and lung are the most favorable sites. The major prognostic factor that significantly affects patient survival is the presence of liver metastases. Their presence indicates a poor prognosis compared to patients without liver metastases [2]. Thirty to eighty percent of patients with gastroenteric and pancreatic tumors initially present with liver metastases [3]. The impact of liver metastases on patient survival depends on the primary tumor site. The primary tumor site remains unknown in 5–10% of patients who initially present with liver metastases.

Radiology has a very critical role in the diagnosis and management of NETs. Although somatostatin receptor scintigraphy, magnetic resonance imaging (MRI), and Gallium-68 (68 Ga) positron emission tomography (PET CT) have been shown to be the more precise tools for the diagnosis of hepatic metastases [4–7], computerized tomography (CT) remains crucial for patient's staging. With its excellent spatial and time resolution, a plethora of information can be provided by multidetector computed tomogaphy (MDCT), including localization and extension of the primary tumor, presence and extent of the liver involvement, and depiction of extrahepatic metastases.

Many studies in the literature have investigated the role of computerized tomography in the evaluation of NETs while a few of them have examined multiphasic CT features of the neuroendocrine tumor liver metastases [8–11]. Most of these studies have shown that most NET liver metastases are hyperattenuating on arterial phase and hypoattenuating on portal venous images; therefore, a dual phase CT is more reliable than a single phase CT in identifying arterial phase hyperenhancement liver metastases [8–11]. Most of these studies regarded the enhancement pattern of all NETs as similar regardless of the primary tumor's origin [2]. Differentiation of histologic subtypes has not been extensively studied.

To the best of our knowledge, no published studies in the literature have yet focused on comparing the quantitative CT features of different histological subtypes of NET liver metastases. Our study will be the first study in the literature in which lung NET liver metastases are assessed and quantitative CT features of different histologic subtypes of NET liver metastases are evaluated. As the difference in histological subtypes of NET liver metastases results in a different prognosis and management strategy, defining MDCT features of liver metastases from different histological subtypes of NET would help to predict prognosis and also to determine therapy planning [12].

The primary purpose of this present study is to assess and compare the MDCT features of NET liver metastases and to investigate the possibility of predicting the histologic subtype of the primary tumor.

Materials and methods

Study design

The Institutional Ethics Committee approved this retrospective study protocol and waived informed consent. The study was conducted in accordance with the principles of the Declaration of Helsinki.

Patient population

Between January 2013 and December 2017, patients with NETs were identified in our institution's database using the Radiology Information System/Picture Archiving and Communication System (RIS/PACS, Centricity 5.0 RIS GE Healthcare). Patients were identified with the search in the PACS system using the word ''neuroendocrine tumor.'' Inclusion criteria consisted of the following: (1) histopathologically proven diagnosis of primary NET, either by biopsy or surgery; (2) the presence of at least one liver metastases, proven by biopsy or surgery; (3) available multiphasic multidetector CT.

We excluded patients who underwent treatment (including systemic chemotherapy and local therapy) before the first available CT and patients, whose primary origin was other than gastroenteric, pancreatic, or lung NET. Patients who had incomplete or inadequate CT images, insufficient image quality, missing medial charts, coexisting malignancies, or marked steatosis were also excluded. For standardization of the tumor grades, patients whose pathological grade according to the Kİ-67 proliferation index was less than 3% were excluded.

CT technique

CT images were acquired using a 64-multidetector CT scanner (Toschiba Aquillion 64; Toschiba Medical Systems, Tokyo, Japan). All patients underwent contrast-enhanced triple-phase CT on the same scanner. Scanning parameters included a slice thickness of 5 mm, a reconstruction interval of 1 mm, automatic tube current modulation, 120 kV and a tube rotation time of 0.5 sn. The scanning range was from the dome of the diaphragm to the iliac crest, and the scan direction was cranio-caudal. Patients fasted for 8 h before the scanning. Patients received 2 mL/kg of non-ionic iodinated contrast medium at 350 mg/mL iodine intravenously through a 22-gauge catheter into the antecubital vein at a rate of 3.5 mL/s by automatic power injector. All cases were acquired using

a standardized multiphasic liver CT protocol that did not change during the course of the study. The protocol was as follows: arterial, portal, and hepatic venous phases were obtained at 35 s, 70 s, and 150 s respectively after the intravenous injection of contrast.

Image analysis

All images were analyzed retrospectively by two abdominal radiologists with 5 and 8 years of experience in abdominal imaging. Disagreements between the readers were resolved by consensus after reassessment of the images together. The reviewers knew that all liver lesions were NET metastases but they were blinded to the clinical data and histological subtypes. The readers were asked initially to evaluate the size, number, and location (focal, diffuse, multifocal) of each lesion. Liver metastases that numbered more than 30 were defined as uncountable. Secondly, readers evaluated the enhancement patterns of each lesion on arterial, portal, and delayed venous phases separately. Tumor attenuation was compared to the surrounding liver parenchyma. Lesions were characterized as "hyperattenuating," "isoattenuating," or "hypoattenuating." Readers noted the best phase, in which metastases were most conspicuous. Readers were also asked to determine the tumor enhancement as homogeneous enhancement (both the periphery and the center of the tumor enhances higher than the liver), peripheral enhancement (periphery of the mass enhances higher than the surrounding liver while central enhancement is relatively lower), or heterogeneous enhancement.

For quantitative analysis, CT attenuation of tumors, liver parenchyma, and aorta were measured using a circular region of interest (ROI) on arterial, portal, and delayed venous phases for reflecting the blood supply of the tumor. The same sized ROIs were placed on all three phases by copying the same ROI from one image to the other. The following parameters were calculated: tumor-to-aorta ratio [T–A = (Tumor–Aorta)/Aorta] in arterial phase (T–A/AP), portal venous phase (T–A/PVP) and delayed venous phase (T–A/HP) and tumor-to-liver ratio [T–L = (Tumor–Liver)/Liver] in arterial phase (T–L/AP), portal venous phase (T–L/PVP) and delayed venous phase (T–L/HP).

Statistical analysis

Descriptive statistics are summarized as counts and percentages for categorical variables; mean and standard deviations for continuous variables. In order to account for intracluster correlation among multiple measurements from the same the patient, Chi square test for clustered data and non-parametric analysis of clustered receiver operating characteristics (ROC) [13] were used. The areas under the ROC curves and 95% confidence intervals for all variables were calculated. Cut-off values were selected by using Youden's Index. Measurements were dichotomized according to cut-off values and sensitivity, specificity, positive and negative predictive values were calculated. A p value of less than 0.05 was considered statistically significant. R version 3.4.2 was used for statistical analysis and clustered ROC function was used.

Results

Clinical characteristics

A total of 255 NET liver metastases in 33 patients divided into three groups; 101 (39.6%) pancreatic, 60 (23.5%) gastroenteric and 94 (36.8%) lung NET liver metastases were analysed. The clinical characteristics of the patients are shown in Table 1.

Difference of CT features between histologic subtypes

There was a significant difference between the size of the subtypes, where the gastroenteric NET liver metastases were significantly larger (38.1 ± 32 mm; $p < 0.001$) than pancreatic NET liver metastases (16.6 ± 17.5 mm) and lung NET liver metastases (15.3 ± 8.4 mm).

Tumor characteristics and enhancement patterns

Contrast enhancement of lesions was homogeneous in 78% of patients ($n = 199$), which was significantly more frequent in patients with cancers of pancreatic origin than in those with cancers of gastroenteric origin ($n = 90$, 89.1% vs. $n = 28$, 46.7%; $p < 0.001$). Gastroenteric NET metastases

Table 1 The clinical characteristics of the patients

	Total	Pancreas-NET	GIS-NET	Lung NET
Gender (female)	22 (61%)	9 (81.8%)	9 (64%)	4 (50%)
Age (mean ± SD)	54.4 ± 14.1	54.6 ± 17.3	54.6 ± 11.4	53.7 ± 15.4
Lesion (n)	255	101	60	94
Size	23.6 ± 25.6	16.6 ± 17.5 mm	38.1 ± 32 mm	15.3 ± 8.4 mm
Best visualized phase n (%)		Arterial 100 (99%)	Portal 32 (53.3%)	Portal 55 (58.5%)

frequently showed heterogeneous enhancement, which was significantly higher than in the other two groups (50% vs. 3% and 2%).

On arterial phase images, most of the NET liver metastases ($n=191$, 74.9%) were hyperattenuating, and tumor hyperattenuation was significantly more frequent in the pancreas group ($p<0.001$). To be precise, 100% ($n=101$) of the pancreatic NET metastases and 76.7% ($n=46$) of the gastroenteric NET metastases showed hyperattenuation, and 23.3% ($n=14$) of gastroenteric NET metastases showed isoattenuation relative to the surrounding liver parenchyma. Only 46.8% ($n=44$) of lung NET liver metastases were hyperattenuating on arterial phase.

For the whole cohort 50.9% ($n=130$) of lesions were isoattenuating, 39.2% ($n=100$) were hypoattenuating and 9.8% ($n=25$) were hyperattenuating on portal venous phase. 80.2% ($n=81$) of pancreatic NET metastases showed isoattenuation, and 19.8% ($n=20$) showed hyperattenuation. For the gastroenteric NET group, 76.7% ($n=46$) of the lesions were hypoattenuating, 15% ($n=9$) were isoattenuating, and only 8.3% ($n=5$) were hyperattenuating. Whereas for the lung NET group, 42.6% ($n=40$) were isoattenuating, and 57.4% ($n=54$) were hypoattenuating. On portal venous phase images, the most frequent presentation for the pancreatic group was isoattenuation (80.2%); whereas it was hypoattenuation for the gastroenteric (52.8%) and lung (52%) NET groups.

On delayed venous phase images 155 lesions (60.7%) were isoattenuating, 91 lesions were hypoattenuating (35.6%) and 9 lesions (3.5%) were hyperattuating for the whole group Pancreatic NET metastases mostly showed hyperattenuation 97% ($n=98$), while the more frequent pattern was hypoattenuation for gastroenteric and lung NET metastases (70%, $n=42$ and 51.1%, $n=48$ respectively).

The qualitative image analysis, tumor characteristics and enhancement patterns of NET liver metastases on MDCT are summarized in Table 2.

For the overall population, pancreatic NET metastases were more optimally visualized on arterial images, but gastroenteric and lung NET metastases were mostly noticeable on portal venous images.

Pancreatic NET metastases were mostly hyperattenuating on arterial phase images and isoattenuating on hepatic and portal venous phase images (79.2%, $n=80$) (See Fig. 1). Meanwhile, gastroenteric NET metastases were more frequently hyperattenuating on arterial phase images and hypoattenuating on portal and delayedvenous phase images ($n=28$, 46.7%) (See Fig. 2). The most frequent pattern for lung NET metastases was hypoattenuation on all three phase images ($n=44$, 46.8%) (See Fig. 3). With respect to the location of the primary tumor, the difference in enhancement patterns of the liver lesions was statistically significant ($p<0.001$).

Quantitative CT parameters of NET liver metastases

ROC analysis of clustered data revealed statistically significant differences between pancreatic NET liver metastases, gastroenteric NET liver metastases, and lung NET liver metastases in terms of tumor-to-aorta (T–A) ratio and tumor-to-liver (T–L) ratio ($p<0.001$). Liver metastases of pancreatic NETs were more enhanced than gastroenteric NETs and lung NETs. T–A ratio and T–L ratio on arterial phase (T–A/AP and T–L/AP), portal phase (T–A/PVP and T–L/PVP), and delayed venous phase (T–A/HVP and T–L/HVP) were significantly higher in the pancreatic group. There was also a significant difference in terms of T-L ratio between pancreatic and gastroenteric NET metastases and pancreatic and lung NET metastases on all three phases, but the portal venous phase was the best phase for differentiation in terms of T–L ratio ($p<0.001$). The cut-off value for T–L ratio was -0.096 to differentiate pancreatic versus gastroenteric NET metastases with a sensitivity of 100% and a specificity of 77% on portal phase images. On delayed venous phase

Table 2 Demonstrates the qualitative image analysis of NET liver metastases

	Total $n=255$	PNET $n=101$	GIS-NET $n=60$	Lung NET $n=94$
Arterial phase				
Hyperattenuating	191 (74.9%)	101 (100%)	46 (76.7%)	44 (46.8%)
Isoattenuating	16 (6%)	0	14 (23.3%)	2 (2.1%)
Hypoattenuating	48 (18.8%)	0	0	48 (51.1%)
Portal venous phase				
Hyperattenuating	25 (9.8%)	20 (19.8%)	5 (8.3%)	0
Isoattenuating	130 (50.9%)	81 (80.2%)	9 (15%)	40 (42.6%)
Hypoattenuating	100 (39.2%)	0	46 (76.7%)	54 (57.4%)
Hepatic venous phase				
Hyperattenuating	9 (3.5%)	2 (2%)	0	7 (%7.4)
Isoattenuating	155 (60.7%)	98 (97%)	18(30%)	39 (41.5%)
Hypoattenuating	91 (35.6%)	1 (1%)	42 (70%)	48 (51.1%)

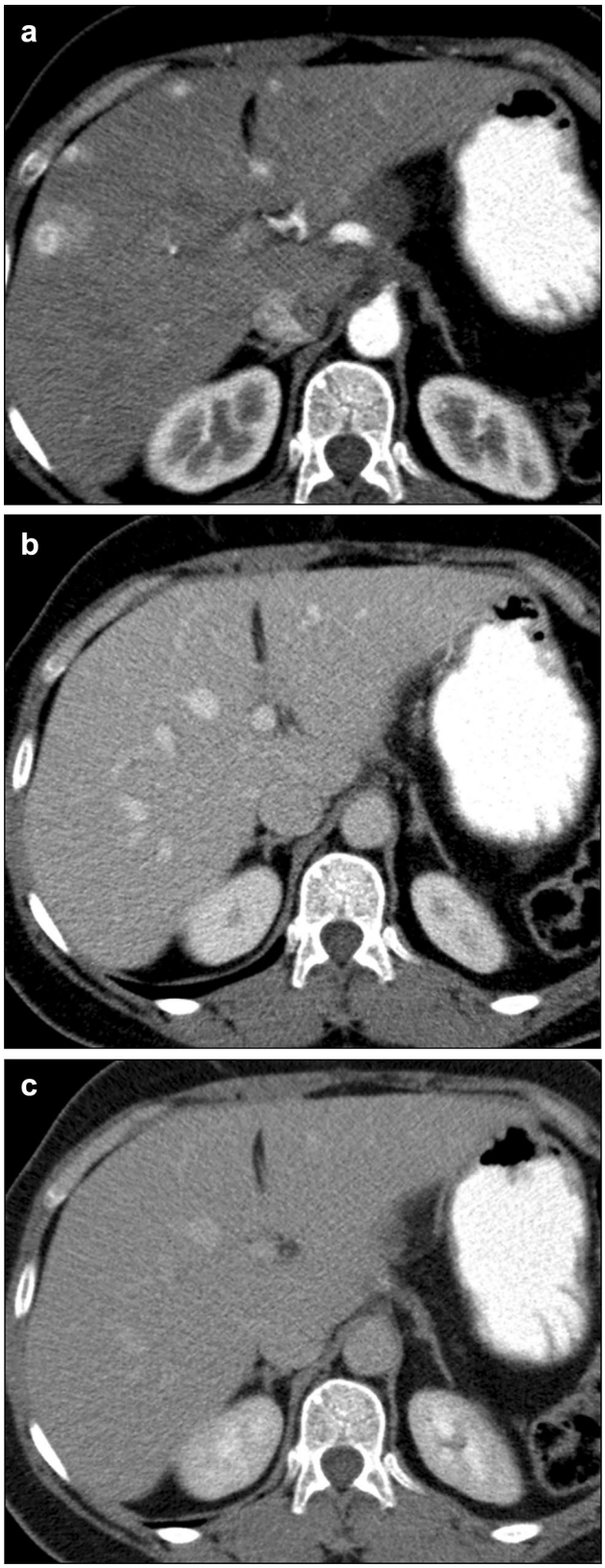

Fig. 1 48-year-old female with pancreatic NET. On multiphasic CT metastatic lesions were hyperdens on arterial phase images (**a**), isodens on portal venous phase (**b**) and isodens on hepatic venous phase images. Lesions were more noticeable on arterial phase images (**a**)

images, the best cut-off value of T–L ratio was −0.078 with a sensitivity of 97% and a specificity of 76.7% for distinguishing the pancreatic from the gastroenteric group. T–L ratio was not significantly different between lung and gastroenteric NET metastases ($p > 0.05$).

T–A ratio can help to differentiate pancreatic and gastroenteric NET metastases on portal and delayed venous phases ($p < 0.001$). The difference in T–A ratio between the two groups on the arterial phase, however, was not significantly different ($p > 0.05$). The ROC curve showed that the best cut-off value of T–A ratio to differentiate pancreatic and gastroenteric NET metastases was −0.292 with a sensitivity of 89% and specificity of 88% on portal venous phase.

T–A ratio was significantly different ($p < 0.001$) in the pancreas and the lung NET subgroups on arterial, portal, and hepatic venous images. In portal venous phase images, the cut-off value for T–A ratio was −0.331 to differentiate pancreas and lung NET metastases with a sensitivity of 95% and a specificity of 80%.

The inter-observer agreement of quantitative image analyses between the two readers was perfect for all quantitative CT features. ICC: 1.000 (%95 CI 0.999–1) for T–A ratio and ICC: 0.999 (%95 CI 0.998–1) for T–L ratio on arterial phase; ICC: 0.999 (%95 CI 0.997–1) for T–A ratio and ICC: 0.999 (%95 CI 0.997–1) for T–L ratio on portal venous phase; ICC: 0.998 (%95 CI 0.993–0.999) for T–A ratio and ICC: 0.999 (%95 CI 0.997–1) for T–L ratio on delayed venous phase. The quantitative CT parameters of NET liver metastases are shown in Table 3.

Discussion

NET liver metastases represent 10% of all hepatic metastatic neoplasms [14]. Due to their relatively slow course, they are very often diagnosed in a progressive stage [15, 16] with the development of liver metastases being the most frequent clinical manifestation [16, 17]. Liver metastases may be associated with a wide spectrum of clinical presentations, from asymptomatic disease incidentally discovered during follow-up to debilitating symptoms caused by carcinoid syndrome and serotonin syndrome. The presence of liver metastases is the most important prognostic factor affecting the survival of patients with neuroendocrine tumors.

The effect of NET liver metastases on a patient's prognosis is related to the site of the primary tumor. Gastrointestinal NETs, for instance, have a five-year survival rate of 60–90%, whereas pancreatic NETs have 30–60% survival rate [18–20]. As a result, the distinction between liver metastases of different histologic subtypes is one of the major diagnostic steps with respect to notable differences in biological behavior and management strategy between the

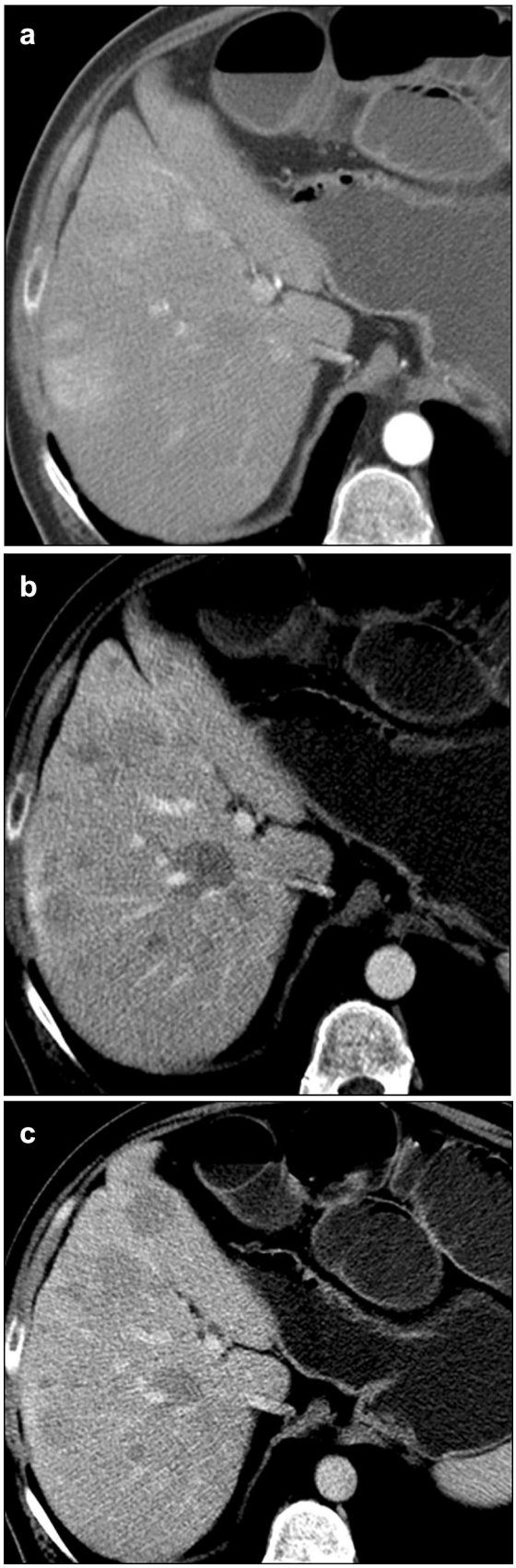

Fig. 2 Neuroendrocrine tumor liver metastasis in a 57-year-old male ▶ patient with gastroenteric primary site. Contrast-enhanced multiphasic CT demonstrated lesions were hyperdens on arterial phase images (**a**), hypodens on portal venous phase (**b**) and hypodens on hepatic venous phase images (**c**)

subgroups. However, 10–13% of all neuroendocrine tumors primary tumor site remains unknown [1, 21].

Imaging plays a crucial role in both the diagnosis and management of NET liver metastases. The role of CT in the assessment of NETs is to help find out the primary site and to discover hepatic and extrahepatic metastases. Because NET liver metastases are highly vascularized tumors, multiphasic CT is more accurate to detect both the primary tumor and liver metastases than a single portal venous phase imaging [22, 23].

The large series of NET liver metastases explored with multiphasic CT in this study shows that the contrast enhancement pattern of hepatic metastases is highly varying. There were significant differences between gastroenteric, pancreatic, and lung NET liver metastases in terms of qualitative and quantitative analysis. Our study is consistent with the literature that most NET liver metastases are hyperattenuating on arterial images (74.9%), but it differs from previous studies in that only 39.2% of the lesions showed washout on portal venous phase [24]. Liver metastases of pancreatic and gastroenteric NETs are usually thought to have similar CT appearances [4], but we found that while most gastroenteric NET liver metastases showed hypoattenuation on portal (76.7%) and hepatic (70%) venous phases, only 1% of pancreatic NET metastases were hypoattenuated. These results, in relation with previous studies, clarify why optimal visualization of most gastroenteric NET liver metastases is in the portal venous phase [9, 22–24].

Our study also confirms that arterial phase imaging is especially important in patients with pancreatic NETs, as most of their liver metastases were isoattenuating on portal phase images (80.2%). The acquisition protocol must include portal and delayed venous phases as well because only 74.9% of total lesions were best visualized, and only 46.8% of lung NET liver metastases were visible, on arterial phase images. We found that portal venous phase was more accurate to diagnose lung and gastroenteric NET liver metastases. Also, on portal and delayed venous images, there were statistically significant differences in terms of quantitative CT parameters that could help to differentiate histologic subtypes. Therefore, we assume that portal and delayed phase images are critical especially in patients with gastroenteric and lung NETs.

To the best of our knowledge, our study is the first study which largely investigates lung NET liver metastases. The enhancement patterns of lung NET liver metastases were challenging, as nearly half of them showed hypoattenuation

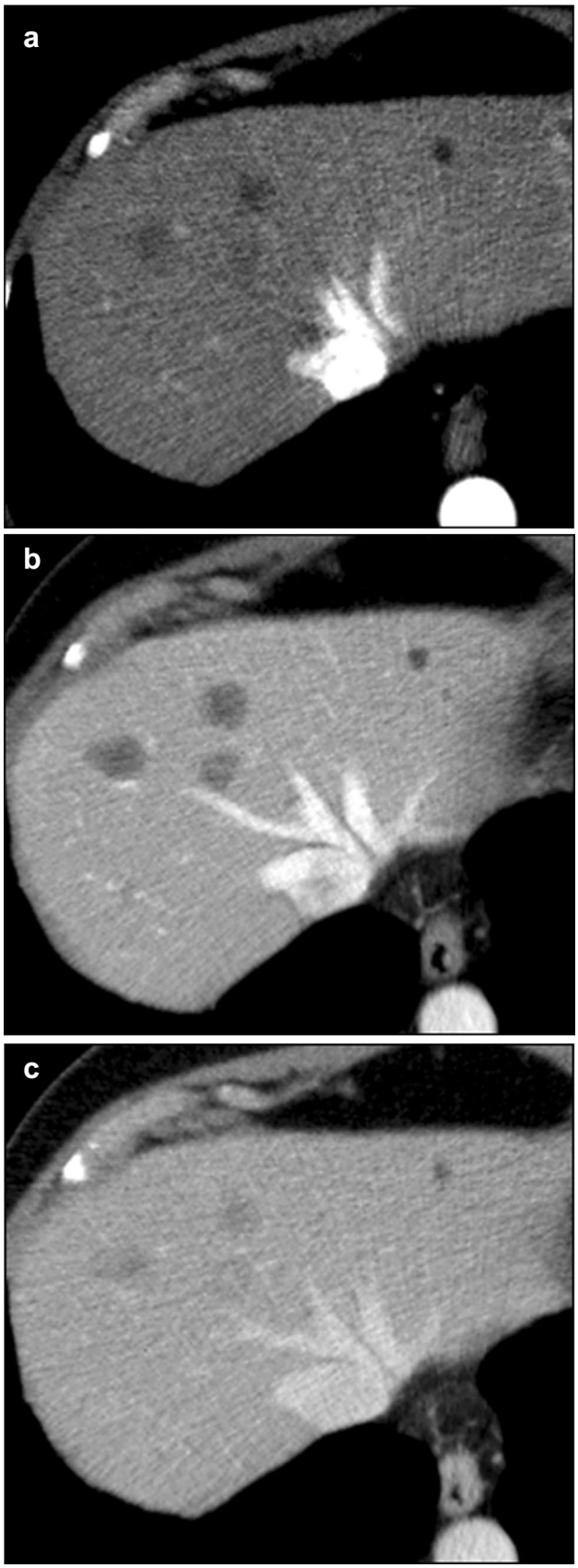

Fig. 3 Neuroendocrine tumor liver metastases in a 70-year-old female patient with lung NET. On contrast-enhanced multiphasic CT liver metastases appeared hypodens on all three phases; arterial phase (**a**), portal venous phase (**b**) and hepatic venous phase images (**c**). Lesions were more clearly visible on portal venous phase (**b**)

on all three phases. This can mimic metastatic disease from other malignancies and further imaging techniques, most importantly Ga 68- DOTATATE-PET CT, may be necessary [6].

The presentation of pancreatic NET liver metastases as hyperattenuated on arterial phase and isoattenuated on portal phase images would be a challenge for differential diagnosis, since benign hepatocelluler lesions such as ''fibronodular hyperplasia'' (FNH) may show a similar enhancement. Therefore, additional imaging techniques, such as Ga 68-DOTATATE-PET CT and MRI using hepatobiliary-specific contrast agents, may be useful [6, 27, 28]. This is especially true because most FNHs are iso/hyperintense on hepatobiliary phase while metastases are hypointense [25–28].

NET liver metastasis from different histological subtypes has different clinical outcomes. Prognosis of NET varies based on the primary tumor site, tumor grade and presence of metastatic disease [18–20]. There are multidisciplinary care treatment options; including somatostatin analogs, targeted therapy, immunotherapy, medical oncology, ablation and embolotherapeutic methods and surgery [2, 12, 15, 19, 20]. If the liver metastasis is not extent, surgery still remains the only curative treatment and metastasectomy should be considered for resectable disease even in patients with non-functional tumors [19, 20]. In diffuse liver involvement, local therapies and surgery are not recommended, and transarterial treatment is required. The principle for transarterial therapies is that most hepatic metastases from NET show arterial phase hyperenhancement. The primary tumor site is one of the predictive factors of tumor response following intra-arterial therapies [29, 30]. Liver metastases from gastroenteric neuroendocrine tumors have a better response than pancreatic tumors. Also for the advanced metastatic disease the development of next-generation multireceptor targeted and radiolabelled somatostatin analogs as well as target-directed therapies can be an alternative. Determination of primary tumor location becomes essential here as the target-directed therapies are only approved in some specific subtypes; like sunitinib has indication in only pancreatic NETs whereas everolimus can be indicated in both gastroenteric and pancreatic subtypes [31, 32]. Therefore, it is very important to determine the primary tumor site to provide an optimal management strategy.

Our study had some limitations. It was a single center and retrospective designed study, however, all patients with NET liver metastases who underwent multiphasic CT were

Table 3 Sensitivity, specificity, positive and negative predictive values for the cut-off values to discriminate between the histological subtypes

Pancreas versus GIS	T/A $p=$	Cut-off	Sensitivity	Specificity	PPV	NPV
Arterial	0.312	N/A	N/A	N/A	N/A	N/A
Portal	<0.001	−0.292	0.89 (0.81–0.93)	0.88 (0.77–0.94)	0.92 (0.87–0.96)	0.82 (0.75–0.88)
Hepatic venous	0.001	−0.265	0.91 (0.83-0.92)	0.78 (0.66–0.86)	0.87 (0.81–0.92)	0.83 (0.77–0.89)
Pancreas vs. GIS	T/L $p=$	Cut-off	Sensitivity	Specificity	PPV	NPV
Arterial	0.034	0.39	0.79 (0.70–0.86)	0.53 (0.40–0.65)	0.74 (0.66–0.80)	0.60 (0.52–0.67)
Portal	<0.001	−0.096	1.00 (0.96–1.00)	0.76 (0.64–0.85)	0.87 (0.81–0.92)	1.00 (0.97–0.99)
Hepatic venous	<0.001	−0.078	0.97 (0.91–0.99)	0.76 (0.64–0.85)	0.87 (0.81–0.92)	0.93 (0.88–0.96)
Pancreas vs. Lung	T/A $p=$	Cut-off	Sensitivity	Specificity	PPV	NPV
Arterial	0.017	−0.66	0.76 (0.67–0.83)	0.80 (0.70–0.87)	0.83 (0.77–0.88)	0.71 (0.64–0.78)
Portal	<0.001	−0.331	0.95 (0.88–0.97)	0.80 (0.70–0.87)	0.86 (0.80–0.91)	0.92 (0.87–0.95)
Hepatic venous	<0.001	−0.249	0.87 (0.79–0.92)	0.72 (0.61–0.81)	0.80 (0.73–0.86)	0.80 (0.74–0.86)
Pancreas vs. lung	T/L $p=$	Cut-off	Sensitivity	Specificity	PPV	NPV
Arterial	0.019	0.187	0.99 (0.94–0.99)	0.54 (0.44–0.64)	0.69 (0.62–0.76)	0.98 (0.94–0.99)
Portal	<0.001	−0.068	0.96 (0.90–0.98)	0.63 (0.53–0.72)	0.74 (0.67–0.79)	0.93 (0.89–0.96)
Hepatic venous	0.015	−0.054	0.92 (0.85–0.95)	0.61 (0.51–0.70)	0.72 (0.65–0.78)	0.87 (0.82–0.92)

chosen, which limits the possibility of a sampling bias. Moreover, all patients included in this study underwent the same CT protocol and basic scan parameters. Although histological proof was received from each patient, some patients had diffuse liver involvement and not all liver metastases were confirmed with histopathological analysis. Third, since there was a low number ($n=1$) in our sample we excluded grade 1 tumors. Finally, because of our strict inclusion criteria (such as lack of treatment before the first available CT, limited primary tumor sites), the number of patients included in the study was limited, but we considered that this was required, as these factors may change the appearance of the lesions.

In conclusion, we observed statistically significant differences in multiphasic CT features (enhancement pattern, T–A ratio, and T–L ratio) between histologic subtypes of NET liver metastases. As the difference in histological subtypes of NET liver metastases results in a different prognosis and different management strategy, these CT features might help to determine the primary tumor site when it is not known to confirm accurate tumor staging and to provide optimal treatment.

Compliance with ethical standards

Ethical approval The Institutional Ethics Committee approved this study protocol.

Conflict of interest The authors declare that they have no conflict of interest.

References

1. Yao JC, Hassan M, Phan A, Dagohoy C, Leary C, Mares JE, Abdalla EK, Fleming JB, Vauthey JN, Rashid A, Evans DB. One hundred years after carcinoid: epidemiology of and prognostic factors for neuroendocrine tumors in 35,825 cases in the United States. J Clin Oncol. 2008;26:3063–72
2. Pavel M, Baudin E, Couvelard A, et al. ENETS Consensus Guidelines for the management of patients with liver and other distant metastases from neuroendocrine neoplasms of foregut, midgut, hindgut, and unknown primary. Neuroendocrinology. 2012;95:157–176
3. S. Scigliano, R. Lebtahi, F. Maire, et al. Clinical and imaging follow-up after exhaustive liver resection of endocrine metastases: a 15-year monocentric experience. Endocr. Relat. Cancer, 2009: 977-99
4. G. d'Assignies, P. Fina, O. Bruno, et al., High sensitivity of diffusion-weighted MR imaging for the detection of liver metastases from neuroendocrine tumors: comparison with T2-weighted and dynamic gadolinium-enhanced MR imaging, Radiology, 2013: 390–399.
5. C. Dromain, T. de Baere, E. Baudin, et al., MR imaging of hepatic metastases caused by neuroendocrine tumors: comparing four techniques, AJR Am. J. Roentgenol. 2003; 180:121–128
6. Alireza Mojtahedi et al. The value of 68Ga-DOTATATE PET/CT in diagnosis and management of neuroendocrine tumors compared to current FDA approved imaging modalities: a review of literature, Am J Nucl Med Mol Imaging 2014;4:426-434
7. C. Dromain, T. de Baere, J. Lumbroso, et al., Detection of liver metastases from endocrine tumors: a prospective comparison of somatostatin receptor scintigraphy computed tomography, and magnetic resonance imaging, J. Clin. Oncol. 2005; 23:70–78
8. A.G. Rockall, R.H. Reznek, Imaging of neuroendocrine tumours (CT/MR/US). Best practice & research, Clin. Endocrinol. Metab. 2007; 21:43–68.
9. E.K. Paulson, V.G. McDermott, M.T. Keogan, D.M. DeLong, M.G. Frederick, R.C. Nelson, Carcinoid metastases to the liver: role of triple-phase helical CT, Radiology 1998; 206: 143–150.

10. W.D. Foley, T.A. Mallisee, M.D. Hohenwalter, C.R. Wilson, F.A. Quiroz, A.J. Taylor, Multiphase hepatic CT with a multirow detector CT scanner, AJR Am. J. Roentgenol. 2000; 175:679–685.
11. I.M. Danet, R.C. Semelka, P. Leonardou, et al., Spectrum of MRI appearances of untreated metastases of the liver, AJR Am. J. Roentgenol. 2003; 181: 809–817.
12. P. Kunz, D. Lagunes, L. Anthony et al, Consensus Guidelines for the Management and Treatment of Neuroendocrine Tumors, Pancreas 2013; 42: 557-577
13. Obuchowski NA. Nonparametric analysis of clustered ROC curve data. Biometrics. 1997: 567-578
14. Benevento A, Boni L, Frediani L. Result of liver resection as treatment for metastases from noncolorectal cancer. J Surg Oncol 2000; 74:24-29
15. Steinmuller T, Kianmanesh R, Falconi M et al. Consensus guidelines for the management of patients with liver metastases from digestive (neuro)-endocrine tumors: foregut, midgut, hindgut, and unknown primary. Neuroendocrinology 2008;87:47-62.
16. Alagusundaramoorthy SS, Gedaly R. Role of surgery and transplantation in the treatment of hepatic metastases from neuroendocrine tumor. World J Gastroenterol 2014;20:14348-58.
17. Kennedy A, Bester L, Salem R, Sharma RA, Parks RW, Ruszniewski P; NET-Liver-Metastases Consensus Conference. Role of hepatic intra-arterial therapies in metastatic neuroendocrine tumours (NET): guidelines from the NET-Liver-Metastases Consensus Conference. HPB (Oxford) 2015;17:29-37.
18. Singh S, Asa SL, Dey C, et al. Diagnosis and management of gastrointestinal neuroendocrine tumors: An evidence-based Canadian consensus. Cancer Treat Rev. 2016;47:32–45.
19. Öberg K, Knigge U, Kwekkeboom D, et al. Neuroendocrine gastro-entero-pancreatic tumors: ESMO Clinical Practice Guidelines for diagnosis, treatment and follow-up. Ann Oncol 2012;23
20. Sundin A, Vullierme MP, Kaltsas G, et al. ENETS Consensus Guidelines for the Standards of Care in Neuroendocrine Tumors: radiologic examinations. Neuroendocrinology. 2009;90:167–83.
21. L. Catena, E. Bichisao, M. Milione, et al., Neuroendocrine tumors of unknown primary site: gold dust or misdiagnosed neoplasms, Tumori 2011;97 :564–567.
22. J.H. Oliver 3rd, R.L. Baron, M.P. Federle, B.C. Jones, R. Sheng, Hypervascular liver metastases: do unenhanced and hepatic arterial phase CT images affect tumor detection, Radiology, 1997;205:709–715.
23. J.H. Oliver 3rd, R.L. Baron, M.P. Federle, H.E. Rockette Jr., Detecting hepatocellular carcinoma: value of unenhanced or arterial phase CT imaging or both used in conjunction with conventional portal venous phase contrast-enhanced CT imaging, AJR Am. J. Roentgenol. 1996;167:71–77.
24. M. Ronot, F. Cuccioli, M. Dioguardi Burgioa, Neuroendocrine liver metastases: Vascular patterns on triple-phase MDCT are indicative of primary tumor location. European Journal of Radiology 2017; 89:156–162.
25. W. Wang, L.D. Chen, M.D. Lu, et al., Contrast-enhanced ultrasound features of histologically proven focal nodular hyperplasia: diagnostic performance compared with contrast-enhanced CT, Eur Radiol. 2013; 23 :2546–2554.
26. V. Roche, F. Pigneur, L. Tselikas, et al., Differentiation of focal nodular hyperplasia from hepatocellular adenomas with low-mecanical-index contrast-enhanced sonography (CEUS): effect of size on diagnostic confidence. Eur Radiol2015 Jan;25:186-95
27. C. Rousseau, M. Ronot, E. Sibileau, et al., Central element in liver masses, helpful, or pitfall? Abdom Imaging. 2015 Aug;40:1904-25.
28. M.D. McInnes, R.M. Hibbert, J.R. Inacio, N. Schieda, Focal nodular hyperplasia and hepatocellular adenoma: accuracy of gadoxetic acid-enhanced MR imaging-a systematic review, Radiology. 2015 ;277:927
29. A. Roche, B.V. Girish, T. de Baere, et al., Prognostic factors for chemoembolization in liver metastases from endocrine tumors, Hepatogastroenterology,2004;51:1751–1756.
30. F. Marrache, M.P. Vullierme, C. Roy, et al., Arterial phase enhancement and body mass index are predictors of response to chemoembolisation for liver metastases of endocrine tumours, Br. J. Cancer 2007; 96: 49–55.
31. Aura D. Herrera Martínez, et al. Targeted Systemic Treatment of Neuroendocrine Tumors: Current Options and Future Perspectives, Drugs (2019) 79:21–42.
32. M. E. Pavel, et al. Efficacy of everolimus plus octreotide LAR in patients with advanced neuroendocrine tumor and carcinoid syndrome: final overall survival from the randomized, placebo-controlled phase 3 RADIANT-2 study Annals of Oncology 28: 1569–1575, 2017